Adaptive Backstepping Control for Hypersonic Vehicles with Actuator Amplitude and Rate Saturation

XIANG Kai, *DU Yanli**, *ZHANG Peng*, *LIN Haibing*

College of Astronautics, Nanjing University of Aeronautics and Astronautics, Nanjing 211106, P. R. China

Abstract: This paper presents a constrained control strategy for the hypersonic vehicle with actuator amplitude, rate constraints and aerodynamic uncertainties. First, a vehicle-actuator control model is derived in consideration of actuator dynamics properties explicitly. Second, a nonlinear disturbance observer is designed to estimate the aerodynamic uncertainties, and then an adaptive backstepping control technique is adopted with a modified first-order-filter to eliminate the "explosion of terms" problem. Next, for handling the actuator amplitude and rate constraints, a novel auxiliary compensation system is constructed to generate quickly compensating signals to ensure tracking performance of command signal. By the Lyapunov stability proof, the proposed control scheme can enssure that the tracking errors converge to an arbitrarily small neighborhood around zero when the actuator constraints and aerodynamic uncertainties exist. Finally, numerical simulations are implemented to illustrate the effectiveness of the proposed control method.

Key words: hypersonic vehicle; amplitude and rate saturation; adaptive backstepping; aerodynamic uncertainty

CLC number: V249.1   **Document code:** A   **Article ID:** 1005-1120(2019)02-0242-11

0 Introduction

The research on control method and technology of hypersonic vehicles (HSVs) has attracted tremendous attention in recent years. One of the major causes is the challenge that HSVs have complex nonlinear aerodynamic characteristics in the flight envelope, always accompanied by model uncertainties, elastic deformation (airframe), and strong coupling of control channels[1]. Besides, performing large angle attitude maneuvers in the near space may result in the actuator saturation which can violently damage the control performance of the HSVs and even cause the vehicle to enter an unstable state. Therefore, actuator amplitude, rate saturation and aerodynamic uncertainty need to be further studied for the control system of HSVs.

Many advanced control approaches, such as predictive control, sliding mode control, and backstepping control have been employed for tackling the above control problems of HSVs[2]. The backstepping control method is widely used in the attitude control and uncertainty suppression of HSVs[3]. However, the problem of "explosion of terms" still exists and is caused by repeated differentiations of the virtual control law. Many scholars have studied the problem and made gratifying progress[4-6]. Dynamic surface control (DSC) technique by Swaroop[7] is introduced to address this problem. In Ref.[5], a novel robust adaptive dynamic surface controller was adopted for a HSV in the presence of aerodynamics uncertainty and input saturation. A robust adaptive DSC scheme based radial basis function neural function was presented by Zong et al.[6] for control problem with parametric uncertainty and input constraints. Waseem et al.[8] introduced a novel integral filter to DSC design procedure of a HSV to ensure feasibility of tracking performance under

actuator magnitude and rate constraints. In Ref.[9], a second-order sliding mode based integral filter possessed superior noise suppression performance compared to first-order filter. But the saturation or sign function consisting in the second-order-filter always improves damage on performance of control system. So a novel integral filter with smooth hyperbolic tangent function was investigated to ensure the outstanding tracking performance. There is no doubt that it is difficult to measure and estimate the aerodynamic uncertainty caused by the external space and the internal coupling of the vehicle. To enssure high performance and stabilization, the disturbance observer[10] (DO) technique that has been widely used is recommended to cope with the uncertainty. In Refs. [11-12], a DO is developed to estimate the unknown compounded disturbance. It is defined to take account of the unknown nonsymmetric input saturation and the unknkown external disturbance, and shows a great estimation performance.

Additionally, it should be pointed out that the anti-windup auxiliary system is also the object concerned by this paper. The command filter consisting of a first-order filter is a nonlinear method to compensate the default between the control instruction and the deflection of the actual actuator. Investigation of previous studies indicates that there are few literatures[13-15] considering amplitude and rate saturation at the same time, whereas it is obvious that the actuator rate has its limitation, and better maneuverability requires higher actuator rates. In Ref.[15], an anti-saturation control architecture incorporating feedback linearization and disturbance observer was designed to deal with input constraints. However, most studies[15-17] did not involve rate constraints of actuator. In Ref.[13], an adaptive backstepping method based on sampling time was constructed to handle the rate and amplitude constraints of the elevator, but the actuator rate of this method can only oscillate between zero and maximum. Yuan et al.[14] constructd a new adaptive backstepping controller for a class of uncertain multiple-input multiple-output nonlinearity systems with input magnitude and rate saturation, and this controller is not very effective in dealing with strong time-varying nonlinear

system. In Ref.[18], a robust constrained autopilot control was developed to solve the angle of attack constraint and actuator input amplitude and rate constraints by utilizing dynamic surface control and intergral barrier Lyapunov functional technique, but the feasibility check[19] of barrier Lyapunov function is always the difficulty of its design. Therefore, the vehicle attitude control problem with the amplitude and rate saturation of the actuator has not been solved effectively.

Motivated by the results of the above mentioned literatures, this paper proposes a disturbance observer-based adaptive backstepping control (DO-ABC) scheme to cope with the HSV precise and robust attitude control problems that include of actuator amplitude and rate saturation with aerodynamic uncertainty. A vehicle-actuator control model is presented by introducing actuator dynamics into the design procedure of attitude control system for HSVs. An advanced integer filter to handle the "explosion of terms" problem is adopted with the analysis of stability error. A new type of auxiliary compensation system is designed to deal with the problem of actuator amplitude and rate constraints.

1 The HSV Model

The HSV attitude control mathematical model with uncertainty can be written as

$$\dot{\boldsymbol{\Theta}} = f_1(\boldsymbol{\Theta}) + \Delta f_1(\boldsymbol{\Theta}) + g_1(\boldsymbol{\Theta})\boldsymbol{\omega} \qquad (1)$$

$$\dot{\boldsymbol{\omega}} = f_2(\boldsymbol{\omega}) + \Delta f_2(\boldsymbol{\omega}) + g_2(\boldsymbol{\omega})\boldsymbol{M}_0 \qquad (2)$$

where $\boldsymbol{\Theta} = [\alpha, \beta, \sigma]^T$ is the attitude angle vector whose three items represent the angle of attack, sideslip angle and bank angle, respectively; $\boldsymbol{\omega} = [p, q, r]^T$ the vector of angular rates consisting of roll, pitch and yaw rate; $\boldsymbol{M}_0 \in \mathbf{R}^3$ the control moment vector; $\Delta f_1(\boldsymbol{\Theta})$ and $\Delta f_2(\boldsymbol{\Theta})$ are uncertainty terms induced by the uncertainty of aerodynamic parameters and modeling errors. The detailed expressions of $f_1(\boldsymbol{\Theta}), f_2(\boldsymbol{\omega}), g_1(\boldsymbol{\Theta})$ and $g_2(\boldsymbol{\omega})$ are shown as follows

$$f_1(\boldsymbol{\Theta}) = [f_\alpha, f_\beta, f_\sigma]^T \qquad (3)$$

$$g_1(\boldsymbol{\Theta}) = \begin{bmatrix} -\cos\alpha\tan\beta & \sin\alpha\tan\beta & 1 \\ \sin\alpha & \cos\alpha & 0 \\ 0 & -\sin\alpha\sec\beta & 0 \end{bmatrix} \qquad (4)$$

$$f_2(\boldsymbol{\omega}) = \begin{bmatrix} J_x^{-1}(J_y - J_z)qr \\ J_y^{-1}(J_z - J_x)pr \\ J_z^{-1}(J_x - J_y)pq \end{bmatrix} \quad (5)$$

$$g_2(\boldsymbol{\omega}) = \text{diag}(J_x^{-1}, J_y^{-1}, J_z^{-1}) \quad (6)$$

where J_x, J_y and J_z are the main moments of inertia of the three axes, respectively; the detailed expression of f_α, f_β and f_σ and other details are given in Refs.[2,17].

Assumption The uncertainties, $\Delta f_1(\boldsymbol{\Theta})$ and $\Delta f_2(\boldsymbol{\Theta})$, satisfy the following conditions

$$\left\| \Delta f_1(\boldsymbol{\Theta}) \right\| \leqslant \eta_1, \left\| \Delta f_2(\boldsymbol{\Theta}) \right\| \leqslant \eta_2 \quad (7)$$

where η_1 and η_2 are all positive constants, and $\|\cdot\|$ stands for Euclidean norm of vectors.

The control moment M_0 is described as

$$M_0 = g_{f\delta}\boldsymbol{\delta}$$

where the matrix $g_{f\delta}$ is the sensitivity moment distribution matrix; $\boldsymbol{\delta}$ control surface vector and its components are modeled by a group of second-order dynamics for control system, designed as follows

$$\ddot{\delta}_i + \kappa_{2i}\dot{\delta}_i + \kappa_{1i}\delta_i = \kappa_{1i}\delta_{ic} \quad i = 1,2,3 \quad (8)$$

where κ_{1i} and κ_{2i} are the positive constants about actuator dynamic system and always far greater than 1 in reality; δ_{ic} is the control deflection commanded. The actuator, meanwhile, has the following constraints because of physical limits

$$-u_m \leqslant \delta_i \leqslant u_m$$
$$-v_m \leqslant \dot{\delta}_i \leqslant v_m$$

where u_m and v_m are the lower and the upper bounds of the actuator amplitude and the rate-saturation, respectively.

Lemma 1 Define the continuous and positive function $V(t)$ with $\forall t \in \mathbf{R}^+$ and $V(0)$ bounded. If the following inequality holds

$$\dot{V}(t) \leqslant -c_1 V + c_2 \rho(t)$$

where c_1 and c_2 are positive constants, and $\rho(t) \in L_\infty$ is real-valued function, then $V(t)$ is bounded and the solution $x(t)$ is uniformly bounded[20].

Lemma 2 For the positive definite Lyapunov function given blow

$$V(t) = \frac{1}{2} e^{\mathrm{T}}(t)\boldsymbol{Q}(t)e(t) + \frac{1}{2}\bar{\boldsymbol{W}}^{\mathrm{T}}(t)\boldsymbol{\Phi}(t)\bar{\boldsymbol{W}}(t)$$

where $e(t) = x(t) - x_d(t)$ and $\bar{\boldsymbol{W}}(t) = \hat{\boldsymbol{W}}(t) -$

$\boldsymbol{W}(t)$, and constants $\boldsymbol{Q}(t) = \boldsymbol{Q}^{\mathrm{T}}(t)$ and $\boldsymbol{\Phi}(t) = \boldsymbol{\Phi}^{\mathrm{T}}(t)$ are dimensionally compatible positive matrices. If the following inequality is satisfied

$$\dot{V}(t) \leqslant -c_1 V + c_2$$

and accompanied by any given initial compact set

$$S_0 = \left\{ x(0), x_d(0), \hat{\boldsymbol{W}}(0) \big| x(0), \hat{\boldsymbol{W}}(0) \text{finite}, \right.$$
$$\left. x_d(0) \in \Omega_d \right\}$$

then the following conclusions can be obtained[20].

(1) The states and weight of closed-loop system will remain in the compact given by
$$S_1 =$$
$$\left\{ x(t), \boldsymbol{W}(t) \Big| \left\| x(t) \right\| < c_{e\max} + \max_{\tau \in [0,t]} \{ \left\| x_d(t) \right\| \} \right.$$
$$\left. x_d \in \Omega_d, \left\| \hat{\boldsymbol{W}} \right\| \leqslant c_{\hat{W}\max} + \| \boldsymbol{W} \| \right\}$$

(2) The states and weight of closed-loop system will eventually converge to the compact sets given by
$$S_2 =$$
$$\left\{ x(t), \hat{\boldsymbol{W}}(t) \Big| \lim_{t \to \infty} \| e(t) \| = \mu_e^*, \lim_{t \to \infty} \| \bar{\boldsymbol{W}} \| = \mu_w^* \right\}$$

where constants

$$c_{e\max} = \sqrt{\frac{2V(0) + \dfrac{2c_2}{c_1}}{\lambda_{Q\min}}}, c_{\hat{W}} = \sqrt{\frac{2V(0) + \dfrac{2c_2}{c_1}}{\lambda_{\Phi\min}}}$$

$$\mu_e^* = \sqrt{\frac{2c_2}{c_1 \lambda_{Q\min}}}, \mu_{\hat{W}}^* = \sqrt{\frac{2c_2}{c_1 \lambda_{\Phi\min}}}$$

with $\lambda_{Q\min} = \min_{\tau \in [0,t]} \lambda_{\min}(\boldsymbol{Q}(\tau))$, $\lambda_{\Phi\min} = \min_{\tau \in [0,t]} \lambda_{\min}(\boldsymbol{\Phi}(\tau))$.

2 Controller Design and Stability Analysis

In this section, a novel HSV attitude control scheme is proposed to deal with attitude tracking. It guarantee that the attitude angle tracks the reference signal $\boldsymbol{\Theta}_c = [\alpha_c, \beta_c, \sigma_c]^{\mathrm{T}}$ with aerodynamic uncertainty and input constraints.

The traditional hypersonic attitude control did not consider actuator dynamics or actuator input amplitude and rate constraints. But the actual control performance of the vehicle will decline sharply when the actuator is in the state of saturation for a long time. Therefore, actuator dynamic property should

be considered in order to obtain the preferable control performance.

A novel reconfiguration vehicle-actuator model consists of vehicle dynamics and actuator dynamics is described as follows.

Define new state variables, $x_1 = \boldsymbol{\Theta}$, $x_2 = \boldsymbol{\omega}$, $x_3 = \boldsymbol{\delta}$, $x_4 = \dot{\boldsymbol{\delta}}$, and Eqs.(1), (2), (8) are converted to new strict feedback system

$$\begin{cases} \dot{x}_1 = f_1 + \Delta f_1 + g_1 x_2 \\ \dot{x}_2 = f_2 + \Delta f_2 + g_{2f} x_3 \\ \dot{x}_3 = x_4 \\ \dot{x}_4 = -\kappa_1 x_3 - \kappa_2 x_4 + \kappa_1 u \end{cases} \quad (9)$$

where $g_{2f} = g_2 g_{f\delta}$, $\kappa_1 = \text{diag}(\kappa_{11}, \kappa_{12}, \kappa_{13})$, $\kappa_2 = \text{diag}(\kappa_{21}, \kappa_{22}, \kappa_{23})$.

2. 1 DOABC scheme design

In this subsection, the controller for above vehicle-actuator model is designed by combining adaptive backstepping control method with the DO.

For the design goal of tracking the desired command angle, a set of auxiliary variables is defined as

$$\begin{cases} z_1 = x_1 - x_d \\ z_i = x_i - \lambda_{i1} \quad i = 2, 3 \\ z_4 = x_4 - \lambda_{41} - e \end{cases} \quad (10)$$

where x_d is the reference command vector of attitude angle; λ_{i1}, $i = 2, 3, 4$ are the estimation of the designed virtual control variables and will be shown at a later stage; e is an auxiliary variable for solving actuator saturation problem and will be given in following Step 4.

Step 1　First, from Eqs.(9), (10), the time derivative of z_1 is described by

$$\dot{z}_1 = f_1 + g_1 x_2 + \Delta f_1 - \dot{x}_d \quad (11)$$

Ref. [12] suggested a new idea for estimating the uncertainty Δf_1. It is given by

$$\begin{cases} \hat{\Delta f_1} = \boldsymbol{\xi}_1 + k_{f1} z_1 \\ \dot{\boldsymbol{\xi}}_1 = -k_{f1}(f_1 + g_1 + \hat{\Delta f_1} - \dot{x}_d) \end{cases} \quad (12)$$

where $\boldsymbol{\xi}_1$ is the intermediate variable; $\hat{\Delta f_1}$ the estimation of Δf_1; and k_{f1} a positive scalar to be designed.

The first Lyapunov function in Step 1 is employed as

$$V_{11} = 0.5\|\tilde{\Delta f_1}\|^2 \quad (13)$$

where $\tilde{\Delta f_1} = \Delta f_1 - \hat{\Delta f_1}$ is the estimation error of Δf_1.

From Eqs.(7), (8), (12), the derivative of $\dot{V}_{11}$ satisfies

$$\dot{V}_{11} = \tilde{\Delta f_1}^T(\dot{\Delta f_1} - k_{f1}\tilde{\Delta f_1}) \leqslant$$
$$\frac{1}{2}\|\tilde{\Delta f_1}\|^2 + \frac{1}{2}\|\dot{\Delta f_1}\|^2 - k_{f1}\|\tilde{\Delta f_1}\|^2 =$$
$$-\left(k_{f1} - \frac{1}{2}\right)\|\tilde{\Delta f_1}\|^2 + \frac{1}{2}\eta_1^2 \quad (14)$$

The controller is designed as virtual control law x_{2d} to enforce $z_1 \to 0$ and expressed as the following form

$$x_{2d} = g_1^{-1}(-f_1 - \hat{\Delta f_1} - k_1 z_1 + \dot{x}_d) \quad (15)$$

where k_1 is a designed positive constant.

As noted earlier, since the aerodynamic variables are not differentiable and associated with uncertainty, it is difficult to find the derivative of the virtual input Eq. (15). The problem of "explosion of terms" will occur with the increase of extension items.

For these problems, a novel first-order integral tanh filter is employed in this paper to eliminate the differential computation of $\dot{x}_{2d}$. It is described in Ref. [12] as

$$\dot{\lambda}_{i1} = -\frac{y_{i1}}{\tau_{i1}} - \zeta_{i1}\tanh(l_{i1} y_{i1}) \quad (16)$$
$$y_{i1} = \lambda_{i1} - x_{2d}$$

where τ_{i1} is the time constant of the filter; ζ_{i1} and l_{i1} are scale positive constants to be designed.

Remark 1　It is noted that the above proposed second-order filter degenerates into a classical integral filters when the parameter $\zeta_{i1} = 0$. As known to all, the span of tanh function is $[-1, 1]$, so the parameter ζ_{i1} constrains the upper and the lower bounds of the tanh function. It is worth stressing that the hyperbolic tangent function guarantees the smoothness of state variables, and especially the smooth process required by the physical system.

Define the second Lyapunov function in

$$V_{12} = \frac{1}{2}\|z_1\|^2 + \frac{1}{2}\|y_{21}\|^2 \quad (17)$$

From Eqs.(10), (14), (15), Eq. (11) becomes

$$\dot{z}_1 = g_1(z_2 + y_{21}) + \tilde{\Delta f_1} - k_1 z_1 \quad (18)$$

So the time derivative of Eq. (17) is

$$\dot{V}_{12} = z_1^T g_1(z_2 + y_{21}) + z_1^T \tilde{\Delta f_1} - k_1\|z_1\|^2 + y_{21}^T \dot{y}_{21} \quad (19)$$

Step 2 From the definition of second error surface z_2, the time derivative of $\dot{z}_2$ is expressed as

$$\dot{z}_2 = f_2 + g_{2f}x_3 - \dot{\lambda}_{21} \qquad (20)$$

The DO of Δf_2, same as Step 1, is designed as follows

$$\begin{cases} \hat{\Delta}f_2 = \xi_2 + k_{f2}z_2 \\ \dot{\xi}_2 = -k_{f2}(f_2 + g_{2f} + \hat{\Delta}f_2 - \dot{\lambda}_{21}) \end{cases} \qquad (21)$$

where ξ_2 is the intermediate variable; $\hat{\Delta}f_2$ the estimation of Δf_2; and k_{f2} is a positive scalar to be designed.

The Lyapunov function for Eq.(18) is chosen as

$$V_{21} = 0.5\|\tilde{\Delta}f_2\|^2 \qquad (22)$$

where $\tilde{\Delta}f = \Delta f_2 - \hat{\Delta}f_2$ is the estimation error of Δf_2.

Through the similar analysis process with Eq.(14), the time derivative of $\dot{V}_{21}$ is given by

$$\dot{V}_{21} = \tilde{\Delta}f_2^{\mathrm{T}}(\dot{\Delta}f_2 - k_{f2}\tilde{\Delta}f_2) \leqslant$$
$$-\left(k_{f1} - \frac{1}{2}\right)\|\tilde{\Delta}f_2\|^2 + \frac{1}{2}\eta_2^2 \qquad (23)$$

The virtual control law of this step is chosen as

$$x_{3d} = g_{2f}^{-1}(-f_2 - k_2z_2 - \hat{\Delta}f_2 + \lambda_{21} - g_1z_1) \quad (24)$$

where k_2 is a designed positive constant.

The approximate estimation variable λ_{31} can be achieved in a similar way by Eq.(16). The estimation error of the virtual control law x_{3d} is defined as

$$y_{31} = \lambda_{31} - x_{3d} \qquad (25)$$

Define a Lyapunov function candidate

$$V_{22} = \frac{1}{2}\|z_2\|^2 + \frac{1}{2}\|y_{31}\|^2 \qquad (26)$$

From Eqs.(10), (24), (25), Eq.(20) becomes

$$\dot{z}_2 = g_{2f}(z_3 + y_{31}) - g_1z_1 + \tilde{\Delta}f_2 - k_2z_2 \quad (27)$$

So the time derivative of Eq.(26) is described by

$$\dot{V}_{22} = z_2^{\mathrm{T}}g_{2f}(z_3 + y_{31}) - z_2^{\mathrm{T}}g_1z_1 + z_2^{\mathrm{T}}\tilde{\Delta}f_2 -$$
$$k_2\|z_2\|^2 + y_{31}^{\mathrm{T}}\dot{y}_{31} \qquad (28)$$

Step 3 The time derivative of the error z_3 is expressed as

$$\dot{z}_3 = \dot{x}_3 - \dot{\lambda}_{31} = x_4 - \dot{\lambda}_{31} \qquad (29)$$

It is worth noting that the control law can not be completely implemented since the physical constraints of the actual system are unavoidable, such as the magnitude and rate constraints considered in this paper.

Inspired by the research in Refs.[6, 13], a new auxiliary first-order system is constructed to reduce the damnification of the attitude control system due to the saturation of the actuator, given as follows

$$\dot{e} = -k_4e + \zeta_e \tanh(\kappa_1(u - u_c)) \qquad (30)$$

where k_4 and ζ_e are parameters that should be designed according to the requirement of the compensation performance. $\Delta u = u - u_c$ is the error between the actual control input u that is control surface deflection and the desired input u_c designed by the control law which will be given next.

Remark 2 Many auxiliary anti-windup saturation compensation schemes based on filtering idea were proposed[10,21]. A noteworthy problem is that auxiliary system is likely to cause excessive deflection of the actuator, and it is also possible to cause strong bucket vibration of the actuator. So a novel tanh function unite is employed to solve this problem and this idea is enlightened by activation function in deep learning. From Eq.(30), the hyperbolic tangent function is adopted to accelerate the response of the compensation system compared with previous command filters. The parameter ζ_e is used to attenuate the magnitude of auxiliary output and avoid excessive deflection of the actuator. It is known from the response of the traditional first order system that we can get the desired the control performance by selecting the parameters k_4 and ζ_e properly .

Remark 3 It is worth noting that traditional compensation system[6,13,22] design is determined by the characteristics of the system itself. So the compensation signal of the compensation system has a highly relates to the system itself, which will cause uncontrollable size of the compensation signal. The design method of compensation system modified by this paper enhances the autonomy of compensation system design. This method not only ensures good attitude tracking performance, but also effectively solves the problem of actuator rate saturation, and the problem of actuator shake and reverse saturation (RS) (A detailed explanation about RS, is illustrated by the example in section 3) caused by the previ-

ous compensation system.

So the virtual control law is chosen as

$$\boldsymbol{x}_{4d} = (-k_3 \boldsymbol{z}_3 + \boldsymbol{\lambda}_{32} - \boldsymbol{g}_{2f}\boldsymbol{z}_2 - \boldsymbol{e}) \qquad (31)$$

where k_3 is a positive constant. The approximate estimation variable $\boldsymbol{\lambda}_{41}$ can be achieved in the similar way by Eq.(16). The estimation error of the virtual control law $\boldsymbol{x}_{4d}$ is defined as

$$\boldsymbol{y}_{41} = \boldsymbol{\lambda}_{41} - \boldsymbol{x}_{4d} \qquad (32)$$

The Lyapunov function is defined as

$$\dot{V}_3 = \frac{1}{2}\|\boldsymbol{z}_3\|^2 + \frac{1}{2}\|\boldsymbol{y}_{41}\|^2 \qquad (33)$$

From Eqs.(10), (31), (32), Eq.(29) becomes

$$\dot{\boldsymbol{z}}_3 = -k_3 \boldsymbol{z}_3 - \boldsymbol{g}_{2f}\boldsymbol{z}_2 + (\boldsymbol{z}_4 + \boldsymbol{y}_{41}) \qquad (34)$$

So the time derivative of Eq.(33) can be given by

$$\dot{V}_3 = -k_3\|\boldsymbol{z}_3\|^2 - \boldsymbol{z}_3^{\mathrm{T}}\boldsymbol{g}_{2f}\boldsymbol{z}_2 + \boldsymbol{z}_3^{\mathrm{T}}(\boldsymbol{z}_4 + \boldsymbol{y}_{41}) + \boldsymbol{y}_{41}^{\mathrm{T}}\dot{\boldsymbol{y}}_{41} \qquad (35)$$

Step 4 In the final step, the derivative of $\boldsymbol{z}_4$ is given as

$$\dot{\boldsymbol{z}}_4 = \dot{\boldsymbol{x}}_4 - \dot{\boldsymbol{\lambda}}_{41} - \dot{\boldsymbol{e}} \qquad (36)$$

From Eqs.(9), (30), Eq.(36) becomes

$$\dot{\boldsymbol{z}}_4 = -\boldsymbol{\kappa}_2 \boldsymbol{x}_4 - \boldsymbol{\kappa}_1 \boldsymbol{x}_3 + \boldsymbol{\kappa}_1 \boldsymbol{u} - \dot{\boldsymbol{\lambda}}_{41} + k_4 \boldsymbol{e} - \zeta_e \tanh(\boldsymbol{\kappa}_1(\boldsymbol{u} - \boldsymbol{u}_c))$$

When $1 \ll \zeta_e < \min(\boldsymbol{\kappa}_{1i})$, $i < 1,2,3$, using Eq.(10), we have

$$\dot{\boldsymbol{z}}_4 \leqslant -\boldsymbol{\kappa}_2 \boldsymbol{x}_4 - \boldsymbol{\kappa}_1 \boldsymbol{x}_3 + \boldsymbol{\kappa}_1 \boldsymbol{u} - \dot{\boldsymbol{\lambda}}_{41} + k_4(-\boldsymbol{z}_4 + \boldsymbol{x}_4 - \boldsymbol{\lambda}_{41}) - \boldsymbol{\kappa}_1(\boldsymbol{u} - \boldsymbol{u}_c) \qquad (37)$$

So we choose the virtual control law in Step 4.

$$\boldsymbol{u}_c = \boldsymbol{\kappa}_1^{-1}(\boldsymbol{\kappa}_2 \boldsymbol{x}_4 + \boldsymbol{\kappa}_1 \boldsymbol{x}_3 + \dot{\boldsymbol{\lambda}}_{41} - k_4(\boldsymbol{x}_4 - \boldsymbol{\lambda}_{41}) - \boldsymbol{z}_3) \qquad (38)$$

Remark 4 The parameter $\boldsymbol{\kappa}_1$ is related to the performance of actuator. The parameter ζ_e is selected as $\zeta_e < \min(\boldsymbol{\kappa}_{1i})$, which can attenuate the magnitude of compensation signals and accelerate the response of compensation system. The higher value of ζ_e corresponds to a worse smoothness and a faster response speed and vice versa. The actual value is determined by the actual actuator.

Define the Lyapunov function

$$V_4 = \frac{1}{2}\|\boldsymbol{z}_4\|^2 \qquad (39)$$

Due to Eqs.(37), (38), the derivative of Eq.(39) can be acquired

$$\dot{V}_4 \leqslant -k_4\|\boldsymbol{z}_4\|^2 - \boldsymbol{z}_4^{\mathrm{T}}\boldsymbol{z}_3 \qquad (40)$$

Remark 5 The analysis and explanation of the presented algorithm is described by two points.

First, the aim of reconfiguration vehicle-actuator model in Eq.(8) is to capture the amplitude and speed of the actuator. In addition, this cascade system is very suitable to adopt backstepping control method which can effectively unite disturbance observer and compensation system.

Second, employing tanh function to improve the corresponding rate of compensation system is the highlights of this paper. The traditional first-order system is described as $\dot{\boldsymbol{e}} = -k_4 \boldsymbol{e} + \boldsymbol{\kappa}_1(\boldsymbol{u} - \boldsymbol{u}_c)$. The contrast Eq.(30) can be found that the effect of tanh function is to accelerate the feedback of $(\boldsymbol{u} - \boldsymbol{u}_c)$ instead of merely depending on $\boldsymbol{\kappa}_1(\boldsymbol{u} - \boldsymbol{u}_c)$ whose $\boldsymbol{\kappa}_1$ belongs to the parameter of system feature itself and is uncontrollable.

2.2 Stability analysis

To facilitate the stability analysis, we define the Lyapunov function

$$V = \frac{1}{2}\sum_{i=1}^{4}V_i \qquad (41)$$

Using Eqs.(14), (19), (23), (28), (35), Eq.(40) yields

$$V = \frac{1}{2}\sum_{i=1}^{4}\|\boldsymbol{z}_i\|^2 + \frac{1}{2}\sum_{i=1}^{2}\|\tilde{\Delta}\boldsymbol{f}_i\|^2 + \frac{1}{2}\sum_{i=2}^{4}\|\boldsymbol{y}_{i1}\|^2 \qquad (42)$$

The time derivative equation of Eq.(42) is

$$\dot{V} \leqslant -\sum_{i=1}^{2}(k_i - \frac{1}{2})\|\boldsymbol{z}_i\|^2 - \sum_{i=1}^{2}(k_{fi} - 1)\|\tilde{\Delta}\boldsymbol{f}_i\|^2 -$$
$$\sum_{i=3}^{4}k_i\|\boldsymbol{z}_i\|^2 + \sum_{i=1}^{4}\eta_i^2 + \sum_{i=2}^{4}(\boldsymbol{y}_{i1}^{\mathrm{T}}\dot{\boldsymbol{y}}_{i1}) + \boldsymbol{z}_1^{\mathrm{T}}\boldsymbol{g}_1 \boldsymbol{y}_{21} +$$
$$\boldsymbol{z}_2^{\mathrm{T}}\boldsymbol{g}_2 \boldsymbol{y}_{31} + \boldsymbol{z}_3^{\mathrm{T}}\boldsymbol{y}_{41} \qquad (43)$$

From Eq.(16) and the filter error $\boldsymbol{y}_{i1}$, if $\zeta_{i1} > |\dot{x}_{id}|_{\max}$, on the basis of Polycarpou and Ioannou[3], we get

$$\boldsymbol{y}_{i1}^{\mathrm{T}}\dot{\boldsymbol{y}}_{i1} =$$
$$\sum_{i=2}^{4}\left(-\frac{\|\boldsymbol{y}_{i1}\|^2}{\tau_{i1}} - \boldsymbol{y}_{i1}^{\mathrm{T}}\zeta_{i1}\tanh(l_{i1}\boldsymbol{y}_{i1}) - \boldsymbol{y}_{i1}^{\mathrm{T}}\dot{\boldsymbol{x}}_{id}\right) \leqslant$$
$$\sum_{i=2}^{4}\left(-\frac{\|\boldsymbol{y}_{i1}\|^2}{\tau_{i1}} - \boldsymbol{y}_{i1}^{\mathrm{T}}\xi_{i1}\right) \leqslant \sum_{i=2}^{4}\left(-\frac{\|\boldsymbol{y}_{i1}\|^2}{\tau_{i1}} + \rho_{i1}\right) \qquad (44)$$

From the research in Ref.[10], the ultimate form of Eq.(43) is derived as

$$\dot{V} \leqslant -\left(k_i - \frac{1}{2}\right)\|\mathbf{z}_i\|^2 - \sum_{i=3}^{4} k_i \|\mathbf{z}_i\|^2 - \sum_{i=1}^{2} (k_{fi} -$$

$$1)\|\tilde{\Delta}f_i\|^2 + \sum_{i=1}^{2}\eta_i^2 + \sum_{i=2}^{4}\left(-\frac{\|\mathbf{y}_{i1}\|^2}{\tau_{i1}} + \rho_{i1}\right) \quad (45)$$

Eq.(45) can be rewritten as

$$\dot{V} \leqslant -c_1 V + c_2 \tag{46}$$

where $c_1 = \min\left\{k_1 - \frac{1}{2}, k_2 - \frac{1}{2}, k_3, k_4, k_{f1} - 1,\right.$

$\left. k_{f2} - 1, \frac{1}{\tau_{21}}, \frac{1}{\tau_{31}}, \frac{1}{\tau_{41}}\right\}, c_2 = \sum_{i=1}^{2}\eta_i^2 + (\rho_{i1}).$

By the differential inequality in Eq.(46), the solution can be obtained as

$$0 \leqslant V(t) \leqslant \frac{c_2}{c_1} + \left(V(0) - \frac{c_2}{c_1}\right)\exp(-c_1 t) \tag{47}$$

According to Lemmas (1, 2), the estimation error of the DO can converge to the following compact set

$$S_{\tilde{\Delta}f_i} = \left\{\|\widetilde{\Delta}f_i\|\Big|\|\widetilde{\Delta}f_i\| < \sqrt{\frac{c_2}{c_1} + V(0)}\right\} \tag{48}$$

The convergence domain of z_i is given in a similar way

$$S_{z_i} = \left\{\|\mathbf{z}_i\|\Big|\|\mathbf{z}_i\| < \sqrt{\frac{c_2}{c_1} + V(0)}\right\} \tag{49}$$

From Eqs.(48,49), the command angle errors can converge to arbitrarily small neighborhoods around zero by properly choosing parameters c_1 and c_2 which can guarantee the stability of vehicle-actuator control system.

3 Simulation

To verify the effectiveness of the proposed control scheme, several simulations are carried out in this section. The winged-cone simulation model, a widely used simulation model of verification actuator constraints, is used to verify the effectiveness of the attitude control system proposed in this paper. The desired attitude command is expressed as $\boldsymbol{\Theta}_c = [\alpha_c, \beta_c, \sigma_c]^T$. The initial attitude and attitude angular rates are chosen as $\boldsymbol{\Theta}_o = [0,0,0]^T$ and $\boldsymbol{\omega}_o = [0,0,0]^T$, respectively. The parameters of actuator dynamics[23] are chosen as $\kappa_{1i} = 900$ and $k_{2i} = 35$. The deflection angles and angular rate of control surfaces are limited within $\pm30°$, ±100 °/s, respec-

tively. Other parameters of control scheme proposed in this paper are as follows: $k_1 = 9.1, k_2 = 0.9, k_3 = 15, k_4 = 5.7, k_{f1} = 2.5, k_{f2} = 4, \zeta_{i1} = 1, \zeta_e = 77, l_{i1} = 0.5, \tau_{i1} = 0.06$. Other initial states about this vehicle are $H_0 = 40$ km, $\tau = 118.5°, \delta = 32°, V_0 = 3$ km/s, $\chi_0 = 0°$ and $\gamma_0 = 0°$.

In simulations tests, a first-order filter is adopted to smooth the reference signals

$$\frac{x_r}{x_c} = \frac{1}{T_r x + 1}$$

where x_r, x_c and T_r are output state of the filter, input command and time parameter, respectively. The selection of the parameters T_r is related to the dynamic performance of the control system. In consideration of the control system design of this paper, it is appropriate to set $T_r = 2$.

In order to compare the control effect, a conventional adaptive dynamic surface control scheme (ADSC) with parameter estimation and actuator compensation in Ref.[21] is used in the simulation tests. Ref.[21] proposed the control scheme ADSC focusing on the flight longitudinal control problem of an HSV with aerodynamic uncertainties and input constraints. The main difference between the two schemes is that the DOABC uses tanh function to design auxiliary compensation system. So the two have the same simulation parameters except ζ_e. Next, the control architectures DOABC and ADSC are tested in two cases, the normal and the uncertainty case. There are 16 design parameters of the controller and the observer in the simulation system and the calculation during one step time is non-iterative. The computer we used is Intel I5 processor, 1.8 GHz. The fourth order method of Runge-Kutta based on MATLAB is used. The simulation step size is 0.02 s. The simulation time is set as 40 s. The actual average running time of 2 000 steps is about 18.57 s. Therefore, it shows that the control method presented is suitable for real-time computation of flight control computer.

3.1 Case 1: Normal case

First, the normal cases of the ADSC and DOABC are implemented to test the dynamic performance when the actuator is within the range of con-

straints.

The corresponding results with attitude tracking and the amplitude and rate of actuator deflection are shown in Figs. 2—4. Fig. 1 shows the three‑dimensional trajectory of the maneuvering flight of a vehicle. As depicted in Fig2, the attitude angles stably follow the desired commands Figs. 3—4 show the difference between the amplitude and the rate of actuator deflection of the two control architectures.

Fig. 2 demonstrates the deflection of actuator amplitude. The third subgraph of Fig.2 shows actuator deflection of control scheme ADSC and DO‑ABC. It is obvious that the actuator is accompanied by obvious bucket vibration for ADSC. However, it should be noted that the rapid deflection may cause the excessive wear of the actuator and other adverse damage for the vehicle. From the comparison above, we can see that the deflection of actuator of the control scheme DOABC shows better smoothness. A similar situation prevails in Fig. 3. Severe rate changes are most likely to cause actuator failure. The architecture and new algorithm DOABC
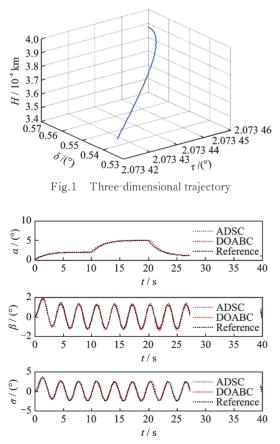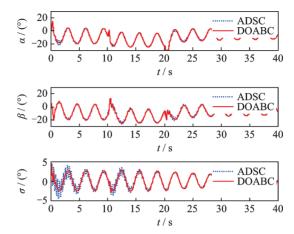

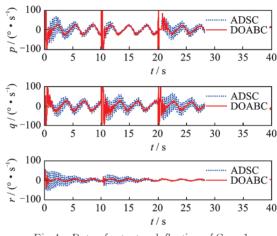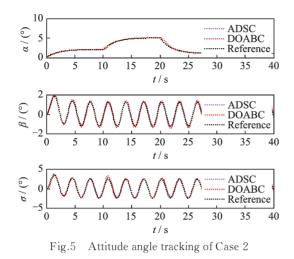Fig.3　Amplitude of actuator deflection of Case 1

Fig.4　Rate of actuator deflection of Case 1

proposed in this paper effectively avoid this situation. The actuator's rate change is smoother. It also shows the effectiveness of the architecture and algorithm proposed in this paper when dealing with the amplitude and rate saturation of the actuator.

3.2　Case 2: Uncertainty case

In this section, the dynamic performance of ADSC and DOABC is tested to validate the aggregation effect of aerodynamic uncertainty and actuator constraints. Therefore, the aerodynamic uncertainty in simulation is selected as $\pm 20\% |f_i|$ randomly. With the same input command, Figs. 5—7 show the attitude angle tracking effect and the deflection of the amplitude and rate of the actuator. Fig. 5 shows that the tracking performance of two control architectures is great and stable. It can be seen that the two architectures have good results in dealing with uncertainty suppression. The tremendous difference in actuator deflection is shown in

Fig.1　Three-dimensional trajectory

Fig.2　Attitude angle tracking of Case 1

Fig.5   Attitude angle tracking of Case 2

Figs.6—7.

The actuator amplitude of control scheme AD-SC exhibits a violent shake in a small range, as shown in Fig.6. The strenuous bucket vibration of the actuator not only brings wear to the actuator, but also leads to the instability and even damage of the vehicle. Instead, the actuator deflection of the
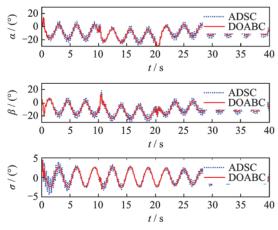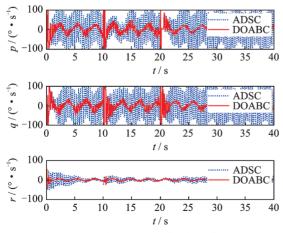

Fig.6   Amplitude of actuator deflection Case 2

Fig.7   Rate of actuator deflection of Case 2

control architecture DOABC shows absolute smoothness and almost no shake. This is more evident in Fig.7. We can observe the rate variation of the actuator and its violent behavior that rapid shifts from one side to the other is what we call reverse RS. However, in the control architecture and algorithm proposed in this paper, RS phenomenon which usually occurs at the moment when the angle of attack begins to change occurs only in a few points. In summary, as shown in the Figs.5—7, the control architecture and algorithm presented herein demonstrate superior performance in processing actuator saturation.

Remark 6   We must realize that this shake and the occurrence of reverse RS saturation of the actuator are due to the inadequate design of the previous anti-saturation auxiliary system and the overall control architecture. The new control architecture and algorithm proposed in this paper takes a step forward in solving this problem. Furthermore, we know that only by improving the algorithm and control architecture can we solve this kind of constraint problem further.

4   Conclusions

This paper investigates the actuator amplitude and rate constraint problem occurring at the maneuvering flight of a HSV with aerodynamic uncertainties. An adaptive backstepping based disturbance observer with anti-saturation auxiliary compensation system control strategy is proposed to deal with such problems. Simulation results show that the proposed control architecture has a satisfactory performance in handling actuator amplitude and rate constraints compared with previous algorithms. For future work, as shown in this paper, the tanh function plays a key role, and other applications about it still attract research interests. Besides, the adaptive adjustment of the parameter ζ_e is worth exploring and will be able to improve the control effect of the presented method.

References

[1]   XIAO L P, ZHANG Y, LU Y P. Control-oriented modeling and simulation on rigid-aeroelasticity cou-

pling for hypersonic vehicle[J]. Transactions of Nan-jing University of Aeronautics and Astronautics, 2015, 32(1)：70-80.

[2] CHNEG X L, WANG P, LIU L H, et al. Distur-bance rejection control for attitude control of air-breath-ing hypersonic vehicles with actuator dynamics [J]. Journal Systems and Control Engineering, 2016, 230 (9)：988-1000.

[3] POLYCARPOU M M, IOANNOU P A. A robust adaptive nonlinear control design [J]. Automatica, 1996, 32(3)：423-427.

[4] WANG J M, WU Y J, DONG X M. Recursive ter-minal sliding mode control for hypersonic flight vehicle with sliding mode disturbance observer[J]. Nonlinear Dynamics, 2015, 81(3)：1489-1510.

[5] XU B, HUANG X Y, WANG D W, et al. Dynam-ic surface control of constrained hypersonic flight mod-els with parameter estimation and actuator compensa-tion[J]. Asian Journal of Control, 2014, 16(1)：162-174.

[6] ZONG Q, WANG F, TIAN B L. Robust adaptive dynamic surface control design for a flexible air-breath-ing hypersonic vehicle with input constraints and uncer-tainty[J]. Nonlinear Dynamics, 2014, 78(1)：289-315.

[7] SWAROOP D, HEDRICK J K, YIP P P, et al. Dy-namic surface control for a class of nonlinear systems [J]. IEEE Transactions on Automatic Control, 2000, 45(10)：1893-1899.

[8] WASEEM A B, LIN Y, AMEZQUITA S K. Adaptive integral dynamic surface control of a hyper-sonic flight vehicle[J]. International Journal of Sys-tems Science, 2015, 46(10)：1717-1728.

[9] LI C Y, JING W X, GAO C S. Adaptive backstep-ping‐based flight control system using integral filters [J]. Aerospace Science & Technology, 2009, 13(3)：105-113.

[10] CHEN W H, YANG J, GUO L, et al. Disturbance observer‐based control and related methods：An over-view[J]. IEEE Transactions on Industrial Electron-ics, 2016, 63(2)：1083-1095.

[11] CHEN M, GE S S. Direct adaptive neural control for a class of uncertain nonaffine nonlinear systems based on disturbance observer[J]. IEEE Transactions on Cy-bernetics, 2013, 43(4)：1213-1225.

[12] WANG F, ZOU Q, HUA C C, et al. Disturbance observer‐based dynamic surface control design for a hy-personic vehicle with input constraints and uncertainty [J]. Proc IMechE Part I：Journal Systems and Con-trol Engineering, 2016, 230(6)：522-536.

[13] WANG Y K, LIU Z X, SUN M W, et al. Adaptive backstepping attitude control with disturbance rejec-tion subject to amplitude and rate saturations of the ele-vator[J]. Journal of Aerospace Engineering, 2016, 32 (3)：04016095.

[14] YUAN R Y, YI J Q. Adaptive control for a class of uncertain nonlinear system with input magnitude and rate saturation[C]// International Conference on Intel-ligent Computing & Integrated Systems. Kunming, China：IEEE, 2010：456-459.

[15] AN H, WANG C H, WU L G. Disturbance observer-based anti-windup control for air-breathing hypersonic vehicles[J]. IEEE Transactions on Industrial Electron-ics, 2016, 63(5)：3038-3049.

[16] ZONG Q, WANG F, SU R, et al. Robust adaptive backstepping tracking control for a flexible air-breath-ing hypersonic vehicle subject to input constraint[J]. Journal Aerospace Engineering, 2015, 229(1)：10-25.

[17] CHEN C, ZHU K, MA G F, et al. Adaptive back-stepping control for reentry attitude of near space hy-personic vehicle with input saturation[C]// Proceed-ing of the 35th Chinese Control Conference. Beijing, China：Springer, 2013.

[18] FENG Z X, GUO J G, ZHOU J. Robust constrained autopilot control for a generic missile in the presence of state and input constraints[J]. Optik, 2017, 149(11)：49-58.

[19] TEE K P, GE S S. Control of nonlinear systems with partial state constraints using a barrier Lyapunov func-tion [J]. International Journal of Control, 2011, 84 (12)：2008-2023.

[20] GE S S, WANG C. Adaptive neural control of uncer-tain MIMO nonlinear systems[J]. IEEE Transactions on Neural Networks, 2004, 15(3)：674-692.

[21] HU Q L, YAO M. Adaptive backstepping control for air-breathing hypersonic vehicle with actuator dynamics [J]. Aerospace Science and Technology, 2017, 67 (8)：412-421.

[22] JAY F, MARIOS P, MANU S. Adaptive backstep-ping with magnitude, rate, and bandwidth con-straints：Aircraft longitude control[C]//Proceedings of the American Control Conference. Denver, USA：[IEEE], 2006：3898-3904.

[23] GUO X P, QI R Y. Design of robust trajectory re-shaping for hypersonic vehicle based on NFTET[J]. Journal of Nanjing University of Aeronautics and As-tronautics, 2017, 49(S)：82-88. (in Chinese)

Authors   Mr. **XIANG Kai** received B.S. degree from Department of Mathematics, Harbin University of Science and Technology, and is currently a postgraduate at College of Astronautics, Nanjing University of Aeronautics and Astronautics (NUAA). His research interest is guidance and control of hypersonic vehicles.

Dr. **DU Yanli** received her Ph.D. degree from NUAA in 2011. Now she is an associate professor at College of Astronautics, NUAA. Her research interests include the guidance and control of hypersonic vehicles or reusable launch vehicles.

Mr. **ZHANG Peng** is currently a postgraduate at College of Astronautics, NUAA. His research interest is guidance and control of hypersonic vehicles.

Mr. **LIN Haibing** is currently a postgraduate at College of Astronautics, NUAA. His research interest is guidance and control of hypersonic vehicles.

Author contributions   Mr. **XIANG Kai** completed the algorithm design and experiments, and wrote the manuscript. Dr. **DU Yanli** contributed to the modification and improvement of this paper. Mr. **ZHANG Peng** provided some experiment models. Mr. **LIN Haibing** offered some advice and checked the manuscript.

Competing interests   The authors declare no competing interests.

(Production Editor：Zhang Bei)